

Chiral Symmetry Restoration and Realisation of the Goldstone Mechanism in the U(1) Gross-Neveu Model at Non-Zero Chemical Potential

Ian Barbour^a, Simon Hands^b, John B. Kogut^c, Maria-Paola Lombardo^d, Susan Morrison^b

^a *Department of Physics and Astronomy,*

University of Glasgow, Glasgow G12 8QQ, U.K.

^b *Department of Physics, University of Wales Swansea,*

Singleton Park, Swansea, SA2 8PP, U.K.

^c *Department of Physics, University of Illinois at Urbana-Champaign*

1110 West Green Street, Urbana, IL 61801-3080, U.S.A.

^d *Istituto Nazionale di Fisica Nucleare, Laboratori Nazionali del Gran Sasso,*

*I-67010 Assergi (AQ), Italy **

and

Fakultät für Physik, Universität Bielefeld, Postfach 100 31, D-33501 Bielefeld, Germany

Abstract

We simulate the Gross-Neveu model in 2+1 dimensions at nonzero baryon density (chemical potential $\mu \neq 0$). It is possible to formulate this model with a real action and therefore to perform standard hybrid Monte Carlo simulations with $\mu \neq 0$ in the functional measure. We compare the physical observables from these simulations with simulations using the Glasgow method where the value of μ in the functional measure is fixed at a value μ_{upd} . We find that the observables are sensitive to the choice of μ_{upd} . We consider the implications of our findings for Glasgow method QCD simulations at $\mu \neq 0$. We demonstrate that the realisation of the Goldstone mechanism in the Gross-Neveu model is fundamentally different from that in QCD. We find that this difference explains why there is an unphysical transition in QCD simulations at $\mu \neq 0$ associated with the pion mass scale whereas the transition in the Gross-Neveu model occurs at a larger mass scale and is therefore consistent with theoretical predictions. We note classes of theories which are exceptions to the Vafa-Witten theorem which permit the possibility of formation of baryon number violating diquark condensates.

I. INTRODUCTION

Successful lattice simulations of QCD at nonzero baryon density have yet to be achieved and the fundamental obstacle to success is the fact that standard hybrid Monte Carlo tech-

*Current address

niques do not admit the complex functional measure appropriate to the full theory. The results of the quenched theory are known to be unphysical [1–3]. Attempts have been made to study unquenched QCD at $\mu \neq 0$ using the Glasgow method which involves generating a statistical ensemble via hybrid Monte Carlo at $\mu = 0$, reweighting the observables by the ratio of the fermion determinant at $\mu \neq 0$ to that at $\mu = 0$ and performing a Grand Canonical Partition Function expansion in the fugacity variable $e^{\mu/T}$ to obtain observables for all μ , but the results were not significantly different from the quenched theory. In this paper we study the Gross-Neveu model which is one of the few models amenable to hybrid Monte Carlo simulations at nonzero density. By implementing the Glasgow method in the Gross-Neveu model and comparing observables with those of a standard hybrid Monte Carlo simulation we reveal the limitations of the Glasgow method. The results are relevant to QCD simulations. Work by Stephanov [3] strongly suggests that any nonzero density simulation which incorporates a real path integral measure proportional to $\det(MM^\dagger)$ is doomed to failure due to the formation of a light “baryonic pion” from a quark and a conjugate quark [2,4,5]. Since an earlier simulation [6] of the Gross-Neveu model at $\mu \neq 0$ did not exhibit such a pathology an explanation is required. We provide a solution to this puzzle later in this paper.

Let us briefly review the current status of QCD simulations at nonzero density. In QCD the fermion determinant is complex for chemical potential μ non-zero, therefore generating an ensemble by Monte Carlo at $\mu \neq 0$ is impracticable. The fermion number density, $J_0 = \langle \bar{\psi}\gamma_0\psi \rangle$, measures the excess of quarks relative to anti-quarks and is expected to start to rise from zero at some value, μ_o . This *onset*, μ_o corresponds to the point where the phase of nuclear matter is more energetically favourable than the vacuum state (for which $J_0 \equiv 0$). Chiral symmetry restoration occurs at some critical μ_c and we expect [7] that $\mu_0 \lesssim \mu_c \simeq m_p/3$, where m_p is the proton mass. Quenched simulations, on the other hand, predict $\mu_o \simeq m_\pi/2$ suggesting that in the limit where the bare quark mass $m \rightarrow 0$ chiral symmetry is restored for any $\mu \neq 0$. This result is unphysical because the pion which has baryon number zero, should not couple to the baryon chemical potential.

First attempts to simulate full QCD using the Glasgow method [8] also produced perplexing results [9]. On an 8^4 lattice with bare quark mass $m_b = 0.01$ at $\beta = 5.1$ we found $\mu_o \simeq 0.1$ which differs considerably from the strong coupling analysis [10] prediction $\mu_c \simeq 0.65$ for $\beta = 5.0$. Furthermore the scaling of μ_o with m was consistent with a Goldstone boson controlling the onset. This result has motivated an assessment of the effectiveness of the Glasgow method via its implementation in a simpler model.

Some insight into the effectiveness and the possible problems of the Glasgow method was obtained by a study of QCD at infinite coupling [11], where we compared results obtained by use of the Glasgow method with the quenched and the nearly exact ones available in that limit. Glasgow results for $\mu \simeq m_\pi/2$ were found to reproduce the quenched ones in quantitative detail. This rules out plausible physical explanations of the early Glasgow onset, which include anomalously low baryonic states or thermal excitations of baryons [12] [10]. In the present study the Glasgow results will be compared with an analogous of the quenched results (Toy model) and with the exact results of [6].

In section II we describe in detail the lattice formulation of the 3d GN model including a discussion of the symmetries and the features of the model which make it amenable to lattice simulation by the hybrid Monte Carlo algorithm even at nonzero chemical potential. In

section III we outline the Glasgow Method for the GN model which makes use of eigenvalue symmetry relations to construct a Grand Canonical Partition Function expansion in the fugacity variable. The special feature of the Glasgow method is that in principle it permits simulations using any fixed value of μ in the functional measure in order to obtain observables such as fermion number density for an extensive range of μ values ranging from $\mu = 0$ to $\mu > \mu_c$. By comparison with the hybrid Monte Carlo simulations where the $\mu \equiv \mu_{upd}$ in the functional measure matches the $\mu \equiv \mu_{meas}$ at which the observable is calculated we assess the effectiveness of the Glasgow method within the limits of our statistics. In section III we present the results of our Gross-Neveu simulation using the Glasgow Method and provide a direct comparison with results of a standard hybrid Monte Carlo simulation. In section IV we present results of a Toy Model simulation of the GN model. In the Toy Model the μ in the functional measure is different from the μ at which the observable is calculated. When μ in the functional measure is set to 0, the Toy model is the Gross-Neveu equivalent of a quenched approximation. When μ in the functional measure equals μ at which the observables are calculated, the Toy model is exact. The Toy model results therefore give an insight into the relevance of including the chemical potential into the dynamics. As discussed in [11], the Glasgow method should improve over the quenched/Toy model because of the reweighting. In the low statistics limit, the Glasgow method should reproduce the Toy results, while in the Glasgow method should approach the exact results. Hence the interest of considering both Toy and exact results to understand the effectiveness of the Glasgow method. In Section V of this paper we discuss the current onset, comparing Toy, Glasgow, and HMC results. We will show that these onsets are all controlled by the lowest excitation in the pseudoscalar composite spectrum. In contrast with QCD, this is not the Goldstone pion, but a massive state. In section VI of this paper we consider a question which is not specific to the lattice simulation method but is highly relevant to our understanding of the physics of chiral symmetry restoration. We provide evidence via a hybrid Monte Carlo simulation that the realisation of the Goldstone mechanism in the Gross-Neveu model (specific to theories with four-fermion interactions) is fundamentally different from the familiar mechanism in QCD. We show that the reason for this is that in the Gross-Neveu model the dominant contributions to the Goldstone pion come from the disconnected diagrams. This fact precludes the existence of a light baryonic pion in $\mu \neq 0$ simulations incorporating four-fermion interactions. Finally in section VII we discuss the relevance of our Gross-Neveu model study to QCD simulations at nonzero chemical potential.

II. LATTICE FORMULATION OF THE 3D GN MODEL

The fermionic part of the lattice action we have used for the bosonized Gross-Neveu model with U(1) chiral symmetry is given by [6]

$$S_{fer} = \bar{\chi}_i(x) M_{ijxy} \chi_j(y) = \sum_{i=1}^N \left[\sum_{x,y} \bar{\chi}_i(x) \mathcal{M}_{x,y} \chi_i(y) + \frac{1}{8} \sum_x \bar{\chi}_i(x) \chi_i(x) \left(\sum_{\langle \tilde{x}, x \rangle} \sigma(\tilde{x}) + i\varepsilon(x) \sum_{\langle \tilde{x}, x \rangle} \pi(\tilde{x}) \right) \right] \quad (2.1)$$

Here, χ_i and $\bar{\chi}_i$ are complex Grassmann-valued staggered fermion fields defined on the lattice sites, the auxiliary scalar and pseudoscalar fields σ and π are defined on the dual lattice

sites, and the symbol $\langle \tilde{x}, x \rangle$ denotes the set of 8 dual sites \tilde{x} adjacent to the direct lattice site x . N is the number of staggered fermion species and $1/g^2$ is the four-fermi coupling. The symbol $\varepsilon(x)$ denotes the alternating phase $(-1)^{x_0+x_1+x_2}$. The auxiliary boson fields σ and π are weighted in the path integral by an additional factor corresponding to

$$S_{aux} = \frac{N}{2g^2} \sum_{\tilde{x}} \sigma^2(\tilde{x}) + \pi^2(\tilde{x}). \quad (2.2)$$

The fermion kinetic operator \mathcal{M} at non-zero density is given by

$$\mathcal{M}_{x,y} = \frac{1}{2} [\delta_{y,x+\hat{0}} e^\mu - \delta_{y,x-\hat{0}} e^{-\mu}] + \frac{1}{2} \sum_{\nu=1,2} \eta_\nu(x) [\delta_{y,x+\hat{\nu}} - \delta_{y,x-\hat{\nu}}] + m \delta_{y,x}, \quad (2.3)$$

where m is the bare fermion mass, μ is the chemical potential, and $\eta_\nu(x)$ are the Kawamoto-Smit phases $(-1)^{x_0+\dots+x_{\nu-1}}$.

The model can be simulated using the hybrid Monte Carlo algorithm [13], in which complex bosonic pseudofermion fields Φ are updated using the action $\Phi^\dagger (M^\dagger M)^{-1} \Phi$. After integration over Φ the measure in the functional integral is therefore manifestly real and given by

$$\det(M^\dagger[\sigma, \pi] M[\sigma, \pi]) e^{-S_{aux}[\sigma, \pi]} = \det(\mathcal{M} + \sigma + i\varepsilon\pi) \det(\mathcal{M} + \sigma - i\varepsilon\pi) e^{-S_{aux}[\sigma, \pi]}, \quad (2.4)$$

where we have used the fact the only complex entries of M occur on the diagonal. Therefore the simulation includes N “white” flavors of fermion with positive axial charge (ie. coupling to $+i\pi$), and N “black” flavors with negative axial charge. If we include the global chiral symmetry valid for $m \rightarrow 0$

$$\chi(x) \mapsto \exp(i\alpha\varepsilon(x))\chi(x) \quad ; \quad \bar{\chi}(x) \mapsto \exp(i\alpha\varepsilon(x))\bar{\chi}(x) \quad ; \quad \phi \equiv (\sigma + i\pi) \mapsto \exp(-2i\alpha)\phi, \quad (2.5)$$

then we see that the model at non-zero lattice spacing has the symmetry: $U(N)_V \otimes U(N)_V \otimes U(1)_A$. It is the $U(1)_A$ symmetry (2.5) which is broken, either spontaneously by the dynamics of the system, or explicitly by a bare fermion mass. In the continuum limit, it is possible to recast the model in terms of $N_f = 4N$ flavors of four-component Dirac spinors $\psi, \bar{\psi}$ [14], ie. $N_f/2$ white flavors and $N_f/2$ black; the global symmetry group should enlarge to $U(N_f/2)_V \otimes U(N_f/2)_V \otimes U(1)_A$. The continuum action approximated by (2.1) after integration over the auxiliary fields σ and π is [15]:

$$S_{cont} = \sum_{p=1}^{N_f/2} \left[\bar{\psi}_p^{white} (\not{\partial} + m) \psi_p^{white} + \bar{\psi}_p^{black} (\not{\partial} + m) \psi_p^{black} - \frac{2g^2}{N_f} \left[(\bar{\psi}_p^{white} \psi_p^{white} + \bar{\psi}_p^{black} \psi_p^{black})^2 + (\bar{\psi}_p^{white} i\gamma_5 \psi_p^{white} - \bar{\psi}_p^{black} i\gamma_5 \psi_p^{black})^2 \right] \right]. \quad (2.6)$$

The relevant features of the 3d Gross-Neveu (GN) model for $\mu \neq 0$ studies are that it has a chiral transition with a massless pion in the broken phase and it can be formulated such that the fermion determinant is positive definite for $\mu \neq 0$ [6].

III. GLASGOW METHOD FOR THE 3D GN MODEL

The key feature of the Glasgow Method is that the chemical potential μ_{upd} appearing in the functional measure is fixed to a constant value while the associated observables are calculated at the appropriate μ_{meas} which can be varied at will. The observables are calculated from logarithmic derivatives of a Grand Canonical Partition Function (GCPF) expansion in the fugacity variable $e^{\mu/T}$ where T is the temperature. To compensate for generating the ensemble at fixed μ_{upd} , the observables are “reweighted” by a ratio R_{rw} of fermion determinants. This procedure of reweighting also serves to make the method exact i.e. the expression for the GCPF from which the observables are obtained is formally correct in the limit of infinite statistics. In practice it is necessary to assess the effectiveness of the Glasgow Method via direct comparison with a standard hybrid Monte Carlo simulation in which μ_{upd} is variable and identical to the μ_{meas} appearing in the expression for the observable.

Consider the expression for the GCPF in the Gross-Neveu model:

$$Z(\mu) = \int [d\sigma][d\pi] \det(M(\sigma, \pi, \mu, m)) e^{-S_{aux}} \quad (3.1)$$

where M is the fermion determinant, S_{aux} contains the auxiliary fields σ and π , m is the bare/current quark mass and μ is the chemical potential. The GCPF (for fixed m) can be rescaled and expressed as an ensemble average of $\det M$ at some fixed value $\mu = \mu_{upd}$:

$$Z(\mu) = \frac{\int [d\sigma][d\pi] \frac{\det M(\mu_{meas})}{\det M(\mu_{upd})} \det M(\mu_{upd}) e^{-S_{aux}}}{\int [d\sigma][d\pi] \det M(\mu_{upd}) e^{-S_{aux}}} = \left\langle \frac{\det M(\mu_{meas})}{\det M(\mu_{upd})} \right\rangle \Big|_{\mu_{upd}} \quad (3.2)$$

where angled brackets denote an average over an ensemble generated with chemical potential μ_{upd} , and μ_{meas} is the chemical potential for which the physical observables are to be calculated. Note that for example generating the ensemble at $\mu_{upd} = 0$ would allow us to circumvent the problem of a complex action in a Monte Carlo simulation.

For optimum efficiency of the Glasgow method we require a large overlap between the ensemble generated using $\det M(\mu_{upd})$ in the functional measure and the exact ensemble generated using $\det M(\mu_{meas})$. Let us define a reweighting factor $R_{rw} \equiv \frac{\det M(\mu_{meas}, m)}{\det M(\mu_{upd}, m)}$. The relative magnitude of the factor R_{rw} configuration by configuration gives a measure of the overlap. If there is poor overlap between the simulated ensemble and the true ensemble it is conceivable that only a small fraction of the configurations will contribute significantly to Z (those where R_{rw} is large in magnitude) in which case extremely high statistics would be required to extract sensible results.

The full lattice action for the bosonized GN model with $U(1)$ chiral symmetry is given in (2.1). The functional measure used in the HMC algorithm is $\det(MM^\dagger)$. To formulate the Glasgow Method for this model we express the Dirac fermion matrix, M and a related matrix \hat{M} , in terms of matrices G and V where G contains all the spacelike links while V (V^\dagger) contains the forward(backward) timelike links. Note that for the Gross-Neveu model $\det(M\hat{M}) = \det(MM^\dagger)$.

$$2iM_{xy}(\mu) = Y_{xy} + G_{xy} + V_{xy}e^\mu + V_{xy}^\dagger e^{-\mu} \quad ; \quad -2i\hat{M}_{xy}(\mu) = Y_{xy}^\dagger + G_{xy} + V_{xy}e^\mu + V_{xy}^\dagger e^{-\mu} \quad (3.3)$$

The term describing the Yukawa couplings of scalars to fermions is given (in terms of the auxiliary fields σ and π on dual lattice sites \tilde{x}) by

$$Y_{xy} = 2i(m + \frac{1}{8} \sum_{\langle x, \tilde{x} \rangle} (\sigma(\tilde{x}) + i\varepsilon\pi(\tilde{x})))\delta_{xy}. \quad (3.4)$$

The determinants of these fermion matrices are related to that of the propagator matrix P (following Gibbs [16]):

$$P = \begin{pmatrix} -GV - YV & V \\ -V & 0 \end{pmatrix} \quad (3.5)$$

which is a matrix of dimension $2n_s^2 n_t$ in this model, for a $n_s^2 \times n_t$ lattice. Note that V is an overall factor of P . The inverse of the propagator matrix is

$$P^{-1} = V^\dagger \begin{pmatrix} 0 & -1 \\ 1 & -G - Y \end{pmatrix} \quad \text{and} \quad (P^{-1})^\dagger = \begin{pmatrix} 0 & 1 \\ -1 & -G - Y^\dagger \end{pmatrix} V \quad (3.6)$$

Note that $Y^\dagger = Y^*$

The determinants of P and M are simply related:

$$\begin{aligned} \det(P - e^{-\mu}) &= \begin{vmatrix} -GV - YV - e^{-\mu} & V \\ -V & -1e^{-\mu} \end{vmatrix} \\ &= \det(GVe^{-\mu} + YVe^{-\mu} + e^{-2\mu} + V^2) \\ &= \det((Ge^{-\mu} + Ye^{-\mu} + V^\dagger e^{-2\mu} + V)V) \\ &= e^{-\mu n_s^2 n_t} \det(G + Y + V^\dagger e^{-\mu} + Ve^\mu) \\ &= e^{-\mu n_s^2 n_t} \det(2M) \end{aligned} \quad (3.7)$$

where we have used $\det V = 1$ and $V^\dagger V = VV^\dagger = 1$. Similarly the determinants of \hat{P} and \hat{M} are simply related.

We shall expand $\det(M\hat{M})$ as a polynomial in $e^{n\mu}$ and in so doing we make use of two symmetries of the eigenvalues. First consider the transformation $\Lambda = \begin{pmatrix} 0 & 1 \\ -1 & 0 \end{pmatrix}$ in the space of the propagator matrix. One can easily show that

$$\Lambda(P^{-1})^\dagger \Lambda^\dagger = \begin{pmatrix} -GV - Y^\dagger & 1 \\ -1 & 0 \end{pmatrix} = \hat{P} \quad (3.8)$$

Thus if λ is an eigenvalue of P then $\frac{1}{\lambda^*}$ is an eigenvalue of \hat{P} . The presence of λ^* and $\frac{1}{\lambda}$ in the spectrum then follows from the fact that $\det(M\hat{M})$ is real for arbitrary fugacity.

We now perform our GCPF expansion:

$$\det(M\hat{M}) = e^{2n_s^2 n_t \mu} \det(P - e^{-\mu}) \det(\hat{P} - e^{-\mu}) \quad (3.9)$$

$$= e^{2n_s^2 n_t \mu} \prod_{i=1}^{n_s^2 n_t} (\lambda_i - e^{-\mu}) \left(\frac{1}{\lambda_i} - e^{-\mu} \right) (\lambda_i^* - e^{-\mu}) \left(\frac{1}{\lambda_i^*} - e^{-\mu} \right) \quad (3.10)$$

$$= e^{2n_s^2 n_t \mu} \prod_{i=1}^{n_s^2 n_t} \left(1 - e^{-\mu}(\lambda_i + \frac{1}{\lambda_i}) + e^{-2\mu} \right) \left(1 - e^{-\mu}(\lambda_i^* + \frac{1}{\lambda_i^*}) + e^{-2\mu} \right) \quad (3.11)$$

$$= \prod_{i=1}^{n_s^2 n_t} \left(e^\mu + e^{-\mu} + \lambda_i + \frac{1}{\lambda_i} \right) \left(e^\mu + e^{-\mu} + \lambda_i^* + \frac{1}{\lambda_i^*} \right) \quad (3.12)$$

$$= \sum_{n=0}^{2n_s^2 n_t} a_n (e^\mu + e^{-\mu})^n \quad (3.13)$$

The above GCPF expansion incorporates all of the eigenvalue symmetries of the model. Provided the $\langle a_n \rangle$ are determined to sufficient accuracy, we can measure the averaged characteristic polynomial over the ensemble generated at any fixed $\mu = \mu_{upd}$ using a hybrid Monte Carlo algorithm, and use this to provide an analytic continuation [8] for the GCPF to any non-zero μ . In order to obtain the fugacity expansion we must determine the eigenvalues of $P\hat{P}$.

Since the matrix V is an overall factor of P , consider the effect of multiplying a timelike link by $e^{2\pi i}$. We can perform a unitary transform to spread this over all timelike links so that a new symmetry emerges:

$$V \longrightarrow V \times \text{element of } Z(n_t) \quad (3.14)$$

This is then transferred to the eigenvalues, λ

$$\det(P - \lambda_i) = 0 \quad (3.15)$$

Therefore the eigenvalues themselves have a $Z(n_t)$ symmetry. This $Z(n_t)$ symmetry holds configuration by configuration. As a consequence of this symmetry, the characteristic polynomial for P is a polynomial in $e^{\mu n_t}$ with $(4n_s^2 + 1)$ real coefficients. Thus we obtain an expansion for the GCPF in the fugacity, $e^{\mu/T}$

$$Z \propto \sum_{n=0}^{2n_s^2} \langle a_n \rangle (e^{\mu n_t} + e^{-\mu n_t})^n \equiv \sum_{n=-2n_s^2}^{2n_s^2} e^{-(\epsilon_n - n\mu)/T} \quad (3.16)$$

The major computational task in performing the GCPF fugacity expansion is the determination of all of the eigenvalues of $P\hat{P}$. It is more efficient to diagonalize $(P\hat{P})^{n_t}$ than to diagonalize $P\hat{P}$, therefore we exploit the $Z(n_t)$ symmetry of the eigenvalues. This introduces a $Z(n_t)$ degeneracy of the eigenvalues and effectively reduces the dimension of the matrix to $4n_s^2 n_t$ to $4n_s^2$. Note that although $P\hat{P}$ is a sparse matrix $(P\hat{P})^{n_t}$ will be dense. The expansion coefficients $\langle a_n \rangle$ are evaluated in the simulation and thermodynamic observables can be obtained from derivatives of $\ln Z$. In particular the number density is defined by:

$$\langle J_0(\mu, ma) \rangle \equiv \lim_{n_s \rightarrow \infty} \left[\frac{T}{n_s^2} \frac{\partial \ln(Z(\mu, m))}{\partial \mu} \right] \quad (3.17)$$

and in terms of the GCPF expansion

$$\langle J_0(\mu) \rangle = \frac{\sum_{n=-2n_s^2}^{2n_s^2} n e^{-(\epsilon_n - n\mu)/T}}{\sum_{n=-2n_s^2}^{2n_s^2} e^{-(\epsilon_n - n\mu)/T}}. \quad (3.18)$$

Since the 3d GN $U(1)$ model has a positive definite functional measure we can choose any desired μ_{upd} and investigate the influence of this choice on the observables. Standard

hybrid Monte Carlo (HMC) simulations [6] showed a clear separation of the Goldstone pion mass scale and the critical chemical potential (μ_c) where chiral symmetry was restored i.e. $\mu_c \gg m_\pi/2$. Thus the lattice Gross-Neveu model is an example of a theory where there is no manifestation of a light Goldstone pion carrying non-zero baryon number even when the model is simulated with a real path integral measure proportional to $\det(MM^\dagger)$.

We set out to investigate whether by applying the Glasgow Method for a given μ_{upd} we could obtain from the GCPF expansion coefficients a fermion number density as a function of μ which would match the results of the standard hybrid Monte Carlo simulations. Of particular interest was whether we would observe the discontinuity in the number density at $\mu_c \gg m_\pi/2$ via the Glasgow Method.

We performed standard hybrid Monte Carlo and Glasgow Method simulations on 16^3 lattices at a four-fermi coupling of $1/g^2 = 0.5$ and $m = 0.01$. To minimise the number of GCPF expansion coefficients we simulated the Glasgow Method with $N = 1$ flavours of staggered fermion. (Note that the results in [17] are appropriate to $N = 3$.) In fig 2 we compare number densities from standard hybrid Monte Carlo simulations with $N = 1$ and $N = 3$. For $N = 3$ $\mu_c = 0.725(25)$ while $m_\pi/2 = 0.18(1)$ [6]; however for $N = 1$ there is a shift such that $\mu_c \simeq 0.6$ i.e. fewer fermion flavours implies earlier chiral symmetry restoration.

The simulation results demonstrate that the chemical potential μ_{upd} at which the statistical ensemble is generated has a strong influence on the thermodynamic observables of the simulation. Fig. 3 shows the number density for the standard HMC simulation and for three simulations using the Glasgow method: one for $\mu_{upd} = 0.0$ another for $\mu_{upd} = 0.625(\simeq \mu_c)$ and finally with $\mu_{upd} = 0.65(> \mu_c)$. The discontinuity at μ_c associated with the fermion losing dynamical mass, which is apparent in the standard hybrid Monte Carlo data is not consistently reproduced by the Glasgow algorithm - the results depend strongly on the choice of μ_{upd} . In fact the discontinuity associated with the chiral transition can be extracted from the GCPF expansion coefficients only when $\mu_{upd} \simeq \mu_c$.

In this simple model the constraints on the effectiveness of the reweighting must come from distribution of the σ field. The histograms of measurements of σ for the two different updates are shown in Fig. 5. For $\mu_{upd} = 0$ the sigma field is sharply peaked about a mean value associated with a large dynamical mass whereas for $\mu_{upd} = 0.7$ the distribution is broader although there is still no clear evidence for a two-state signal for a fermion with and without dynamical mass. Despite the absence of a two-state signal in the sigma fields the reweighting still reflects the discontinuity in the fermion number density although this discontinuity is sharper in the standard HMC simulation.

A. Free Gas behaviour

We shall compare J_0 as a function of μ obtained from the Glasgow method with the number density of a lattice gas of free fermions with mass $m_f = m + \langle \sigma \rangle$. Firstly we consider the simulation with $\mu_{upd} = 0.0$ where we found J_0 rises smoothly from μ_o to saturation and secondly we consider the simulation with $\mu_{upd} = 0.625$ where we saw a discontinuity in J_0 at a value of μ which was consistent with the μ_c determined by the standard hybrid Monte Carlo where $\mu_{upd} = \mu_{meas}$ for each value of μ simulated.

This comparison with free lattice gas number density is useful because it gives us a qualitative idea of whether the J_0 obtained for a given μ_{upd} is revealing the transition from the chirally broken phase where m_f is large to the chirally symmetric phase with $m_f \simeq m$. In fact as we shall see in section V the Toy Model number density is very well approximated by a free lattice gas of fermions therefore any significant departure from the free gas behaviour for the Glasgow Method number density must be due to the reweighting factor R_{rw} .

The fermion number density for a free Fermi gas is obtained by summing over the finite set of Matsubara frequencies [18] that arises in the lattice thermodynamics. The appropriate expression for the number density, J_0 in terms of the momentum sums for a 3-dimensional free lattice gas is :-

$$J_{0free} = 2i \int_{-\pi}^{\pi} \frac{d^3p}{2\pi^4} \frac{\sin(p_t + i\mu) \cos(p_t + i\mu)}{\sum_{i=1}^2 \sin^2 p_i + \sin(p_t + i\mu) + m_f^2} \quad (3.19)$$

where p_t is associated with the temporal direction.

Recall that $\langle\sigma\rangle$ is a measure of the physical fermion mass. The results of our J_0 comparison are plotted in Fig. 4. In our GN simulations using the Glasgow method for $\mu_{upd} = 0.0$ the fermion number density was consistent with a gas of free fermions with a dynamical mass $m_f = m + \langle\sigma\rangle|_{\mu=0}$. As we shall describe in section V, this is the same behaviour we observed for the Toy model. However for $\mu_{upd} = 0.625$ there is a clear indication of a *discontinuity* at μ_c and for $\mu > \mu_c$ the results are consistent with a free gas of fermions with dynamical mass $m_b + \langle\sigma\rangle|_{\mu=0.625}$. We found that for $\mu_{upd} = 0.65$ i.e. as the chemical potential in the functional measure increased beyond μ_c the discontinuity disappeared again. This suggests that within the limits of the statistics of a typical lattice simulation, the inclusion of the reweighting term R_{rw} in the expression for the GCPF is insufficient to project onto the ensemble appropriate to μ_{meas} except when $\mu_{meas} \simeq \mu_{upd}$.

B. Lee-Yang Zeros

We have seen that the Glasgow Method fermion number density only gives a reliable estimate for μ_c from the number density when $\mu_{upd} \simeq \mu_c$: however we also expect a signal for criticality from the partition function zeros. According to the theorems of Lee and Yang [19], the phase transitions of a system are controlled by the distribution of roots of the GCPF. A phase transition occurs whenever a root approaches the real axis in the infinite volume limit. In practical lattice simulations we are certainly not close to the thermodynamic limit, however as the lattice volume is increased we expect the zero with the smallest imaginary part to approach the real axis, converging to the critical value of the appropriate parameter. The Lee-Yang zeros in the complex μ plane are the zeros of eqn. (3.1) and their distribution should reflect μ_c . The zeros in the complex μ plane for the $\mu_{upd} = 0.0, 0.5, 0.55, 0.625, 0.65, 0.85$ are plotted in Fig. 6. The first point to note is that the zeros form a distinctive and elaborate pattern. Even for this simple model it would be difficult to predict analytically the distribution of zeros however some very clear features emerge when we compare the distributions appropriate to different μ_{upd} . For $\mu_{upd} < \mu_c$ i.e. $\mu_{upd} = 0.0, 0.5, 0.55$ there is an arc of zeros which intersects the real axis at $\mu \simeq 0.6 \simeq \mu_c$. For these 3 values of μ_{upd} we saw no evidence of a discontinuity in J_0 at $\mu = 0.6$. Now

at $\mu_{upd} = 0.625$ there is clear change in the pattern of zeros. What was an arc of zeros at $\mu \simeq 0.6$ now becomes a broader vertical line and two additional lines of zeros sit outside the main body of the distribution at $\mu \simeq 0.5$. Recall that for $\mu_{upd} = 0.625$ we did see a discontinuity at μ_c in J_0 . As we increase μ_{upd} beyond μ_c i.e. for $\mu_{upd} = 0.65, 0.85$ the vertical line of zeros migrates to higher μ and the main zeros distribution extends further into the low μ region of the complex μ plane. For $\mu_{upd} = 0.85$ the vertical line of zeros sits at $\mu \simeq 0.85$ i.e. far from μ_c .

IV. TOY MODEL VERSUS STANDARD HYBRID MONTE CARLO RESULTS

In this section we discuss an approximate model, which we will refer to as the ‘Toy’ model, which will turn out to give useful insight into the results of Glasgow reweighting applied to the GN model. In the Toy Model the chemical potential used in the measure μ_{meas} can be different from that used in the update μ_{upd} . It can be seen as the equivalent of the quenched approximation when $\mu_{upd} = 0$, and is the exact model when $\mu_{meas} = \mu_{upd}$. It is essentially the Glasgow Method with $R_{rw} \equiv 1$. When $\mu_{upd} = 0$ and the statistics is low, the Glasgow method results coincide with those of the Toy model, and should approach the exact results in the large statistics limit [11].

Let us begin by reviewing what is known about the GN model in the mean field approximation.

In the mean field approximation, which turns out to be the leading order of an expansion of powers of $1/N_f$, we solve for the expectation value of the auxiliary scalar $\langle\sigma\rangle$ self-consistently using the gap equation, which reads (with bare mass m set to zero):

$$\langle\sigma\rangle = -g^2\langle\bar{\psi}\psi\rangle = \frac{g^2}{V}\text{tr}S_F(\langle\sigma\rangle) = \int_p \text{tr}g^2 \frac{1}{i\not{p} + \langle\sigma\rangle}. \quad (4.1)$$

Eqn. (4.1) can be solved using a lattice regularisation [20] and has a non-trivial solution $\langle\sigma\rangle \neq 0$ for $g^2 > g_c^2 \simeq 1.0$. The dynamical fermion mass $m_f = \langle\sigma\rangle$ then defines the model’s physical scale, and there is a continuum limit corresponding to a continuous chiral symmetry restoring phase transition as $\langle\sigma\rangle \searrow 0$, $g^2 \searrow g_c^2$.

The gap equation can also be generalised to $\mu \neq 0$:

$$\langle\sigma\rangle(\mu) = -g^2\langle\bar{\psi}\psi\rangle(\mu) = \frac{g^2}{V}\text{tr}S_F(\mu, \langle\sigma\rangle(\mu)); \quad (4.2)$$

once again the solution can be found, either in the continuum [21], or on a lattice [22] [6]. The salient feature of the solution is that $\langle\sigma\rangle(\mu)$ remains unchanged from its zero-density value $\langle\sigma\rangle(0)$ as μ is increased, up to a critical value

$$\mu_c = \langle\sigma\rangle(0), \quad (4.3)$$

whereupon it falls immediately to zero, signifying that chiral symmetry is restored via a first order transition. Introduction of a small bare fermion mass m causes a slight softening of the transition. The hybrid Monte Carlo simulation results of refs. [22] [6] confirm that this picture is qualitatively correct.

Now consider a 3d GN model in which a value of the chemical potential μ_{upd} is used to generate the ensemble, and a value μ_{meas} to measure expectation values, with $\mu_{upd} \neq \mu_{meas}$ in general. We will refer to this as the ‘Toy model’. Notice that $\mu_{upd} = \mu_{meas}$ defines the standard hybrid Monte Carlo calculation whereas $\mu_{upd} = 0$ is the equivalent of a quenched study (we could indeed refer to the case $\mu_{upd} \neq \mu_{meas}$ as a ‘generalised quenched approximation’).

In a mean field treatment of the Toy model the σ field is constrained to its $\mu = \mu_{upd}$ value, so therefore we simply substitute $\langle \sigma \rangle = \langle \sigma \rangle(\mu_{upd})$ in the fermion propagator, and calculate $\langle \bar{\psi} \psi \rangle$. Therefore the Toy counterpart of eqn.(4.2) is

$$\langle \sigma \rangle(\mu_{upd}) \neq -g^2 \langle \bar{\psi} \psi \rangle(\mu_{meas}) = \frac{g^2}{V} \text{tr} S_F(\mu_{meas}, \langle \sigma \rangle(\mu_{upd})) \quad (4.4)$$

In the mean field approximation, the above considerations suggest that all Toy models are equivalent to free fermion models with $m_f = \langle \sigma(\mu_{upd}) \rangle$. This is confirmed by the numerical simulations described below. It is clear that Glasgow method reweighting cannot work in the GN model because the ensemble generated with $\mu_{upd} < \mu_c$ has zero overlap with that generated using $\mu_{upd} > \mu_c$. This means that all Toy models with $\mu_{upd} < \mu_c$ should be equivalent, and should approximate the standard HMC results for $\mu_{meas} < \mu_c$. However, for $\mu_{meas} \geq \mu_c$ the propagator S_F remains that of a free fermion with $m_f = \langle \sigma \rangle(\mu_{upd})$ i.e. the fermion appears to retain its dynamical mass therefore we cannot expect a chiral symmetry restoring transition in the Toy model. Consider next the Toy model with $\mu_{upd} > \mu_c$. The propagator S_F now always describes a massless fermion, therefore in this case we expect the Toy model to reproduce the exact results only for $\mu_{meas} > \mu_c$.

It is also possible, and instructive, to test these ideas once quantum fluctuations of σ are included. Accordingly we have performed simulations of the Toy model for $\mu_{upd} = 0$, μ_{meas} arbitrary, using the hybrid Monte Carlo algorithm. Fig. 1 compares the results of these simulations with the exact simulation results [6], obtained with the same parameters (coupling $1/g^2 = 0.5$, bare mass $m = 0.01$, lattice size $L = 16$, $N = 3$ corresponding to $N_f = 12$ continuum flavours), and the mean field predictions of (4.4). Both the condensate $\langle \bar{\psi} \psi \rangle$ and number density $\langle J_0 \rangle$ are plotted as functions of μ_{meas} . We see that the Toy model with $\mu_{upd} = 0$ is well described by a massive free field with $m_f = \langle \sigma \rangle(0)$ for $\mu_{meas} < \mu_c \simeq 0.725$, and that exact and Toy results agree well in this range; for $\mu_{meas} > \mu_c$, however, while the exact results for $\langle \bar{\psi} \psi \rangle$ fall steeply, the Toy results exhibit a smooth crossover, approaching zero only for $\mu_{meas} \simeq 1.4$. For $\mu_{meas} > \mu_c$ the full model is better described by a massless free field, corresponding to $\mu_{upd} > \mu_c$, $\langle \sigma \rangle(\mu_{upd}) = 0$, indicating the restoration of chiral symmetry. In all cases the mean field prediction (4.4) reproduces the Toy simulation results well, indicating that quantum fluctuations are small due to the relatively large value of N_f .

We deduce that μ_c is not observable in the Toy model, since there is no chiral symmetry restoration. Note however that the value μ_o at which the onset of $\langle J_0 \rangle$ occurs is the same for both Toy and exact models, reflecting the fact that the onset on a finite lattice (and perhaps even in the thermodynamic limit) is not associated with the chiral transition.

We emphasize that this simple analysis works well because at $1/g^2 = 0.5$ and $N_f = 12$ the fluctuations in σ are highly suppressed. We verified that the microscopic distribution of the σ field is very sharply peaked about its constant value. This condition serves to make the model well approximated by the appropriate free fermion field in each phase. Because the two phases for $\mu < \mu_c$ and $\mu > \mu_c$ are clearly different, we anticipate that Glasgow

reweighting using $\mu_{upd} = 0$ will not be able to capture the chiral phase transition because the overlap between σ distributions from each phase is likely to be very small. The overlap would be exactly zero in the infinite N_f limit where fluctuations are completely suppressed. It would be interesting to repeat this exercise closer to the critical point $g_c^2 \simeq 1$ although at this coupling the chiral transition is more difficult to identify.

V. PSEUDOSCALAR MASS AND REALISATION OF THE GOLDSTONE MECHANISM

Although we have shown that the Glasgow method and the Toy model simulations differ in their quantitative predictions for the number density $J_0(\mu)$ from the standard hybrid Monte Carlo simulations we observe that the *onset*, μ_o in J_0 (ie. the value of μ where J_0 starts to increase from zero which is usually interpreted as the point of chiral symmetry restoration) is correctly predicted by both Toy model and the Glasgow method. This is true even for simulations with modest statistics.

An important result reported in [6] was the numerical proof that $\mu_o \gg m_\pi/2$ in standard hybrid Monte Carlo simulations of the GN model. Thus we had an example of a theory which could be simulated at $\mu \neq 0$ with dynamical fermions and where there were no pathologies associated with the fact that there was a Goldstone pion in the spectrum. In the Gross-Neveu theory even in the Toy model simulations (which are partially quenched) $\mu_o \gg m_\pi/2$ in agreement with the full theory. Why then are there pathologies associated with m_π in QCD? We set out to gain insight into this fundamental difference between the two lattice models.

We shall discover that the onset in J_0 always occurs at $\mu_o = m_{PS}/2$, where m_{PS} is the mass of the pseudoscalar state measured via GG^\dagger where $G(G^\dagger)$ is the fermion (anti-fermion) propagator. In QCD m_{PS} is the Goldstone pion, however in four fermion models the Goldstone mechanism is realized by the auxiliary field $\vec{\pi}$ and m_{PS} is a much heavier state which appears to be close to twice the dynamical fermion mass.

Let us first consider the realisation of the Goldstone mechanism in the Gross-Neveu model. In particular we measure and compare the connected and disconnected contributions to the Goldstone pion. If the pion has a dominant connected contribution we expect a pole in the pseudoscalar propagator corresponding to a light particle with mass $\propto \sqrt{m}$. If, on the other hand, the pion has a dominant disconnected contribution the mass scale corresponding to the pole in the pseudoscalar propagator will be $\simeq 2m_f(\mu = 0) \gg m_\pi$.

Consider the lattice Ward identity for the chiral condensate:

$$\begin{aligned} \sum_y \langle \bar{\psi} \gamma_5 \psi(y) \bar{\psi} \gamma_5 \psi(x) \rangle &= \sum_y \langle \text{tr}(G_{-\mu}^\dagger(x, y) G_{+\mu}(x, y)) \rangle - \langle (\text{tr} \gamma_5 G(x, x)) (\text{tr} \gamma_5 G(y, y)) \rangle \\ &= - \frac{\langle \bar{\psi}(x) \psi(x) \rangle}{m_q} \end{aligned} \quad (5.1)$$

The pion susceptibility Eqn.(5.1) has contributions from a connected channel (1st term) and a disconnected channel (2nd term).

Consider the Dirac kinetic operator \mathcal{D} for staggered fermions. At $\mu = 0$ the relation $\mathcal{D}^\dagger = -\mathcal{D}$ holds. For $\mu \neq 0$ the fact that e^μ ($e^{-\mu}$) multiplies the forward (backward)

timelike gauge links in the lattice action means that $\mathcal{D}^\dagger \neq -\mathcal{D}$, because in the matrix \mathcal{D}^\dagger , $e^{-\mu}$ (e^μ) now multiplies the forward (backward) links. Consequently the propagators G (with $G = M^{-1}$) and G^\dagger are no longer trivially related as they are at $\mu = 0$. Thus the pseudoscalar propagator, G_{ps} , is defined by

$$G_{ps}(t) = \sum_{\vec{x}} G_{+\mu}(\vec{x}, t) G_{-\mu}^\dagger(\vec{x}, t) \quad (5.2)$$

Let λ_{ps} be the smallest eigenvalue of the Gibbs propagator matrix P (eqn. 3.5). It can be shown that λ_{ps} is associated with the mass pole in G_{ps} and that when we consider a single lattice configuration λ_{ps} directly corresponds to a Lee-Yang zero and therefore induces a singularity in J_0 i.e. triggers the rise from zero of the fermion number density. To see this observe that $\det M$ can be simply expressed in terms of the eigenvalues of P and Z can be similarly expressed in terms of its zeros α_i in the e^μ plane:

$$\det M \propto \prod_i (e^\mu - \lambda_i) \quad ; \quad Z \propto \prod_i (e^\mu - \alpha_i). \quad (5.3)$$

Since $Z = \langle \det(M) \rangle$ we see that on a single configuration $\alpha_i = \lambda_i$. Note however that the ensemble averaged α_i 's are not in general the same as the ensemble averages of the λ_i 's.

The number density on a single configuration $J_0^i \sim \partial \ln \det M / \partial \mu$ whereas the ensemble average is given by $J_0 \sim \partial \ln \langle \det M \rangle / \partial \mu$. Clearly the chemical potential where the number density begins to rise from zero on a single configuration will be determined by the numerical value of λ_{ps} (i.e. $\mu_o = \lambda_{ps}$).

It has been proved by Gibbs [16] that if we assume that the pion has a dominant connected contribution it follows that $\lambda_{ps} \sim e^{-\frac{m_\pi}{2}}$. In this case we can only envisage achieving a physically meaningful result ($\mu_o > \frac{m_\pi}{2}$) if $\alpha_i \neq \lambda_i$. However in the exceptional circumstance where the disconnected contribution to the pion is dominant we expect that $\lambda_{ps} \sim e^{-m_f}$ so that configuration by configuration $\mu_o = m_f > \frac{m_\pi}{2}$. In this section we shall prove that in the 3d GN $U(1)$ model the Goldstone pole forms in the disconnected channel therefore the state described by G_{ps} no longer corresponds to the Goldstone pion. Instead we find:

$$G_{ps} \simeq e^{-2m_f(\mu=0)t} \quad (5.4)$$

Since $|\lambda_{ps}|$ will now correspond to the dynamical fermion mass m_f rather than $m_\pi/2$ we have no reason to expect an early onset in the Gross-Neveu model despite the existence of a light Goldstone pion in the spectrum.

In Fig. 7 we have plotted the propagator for the pion (measured from the auxiliary field), the square of the fermion propagator and the pseudoscalar propagator. The results show that the pseudoscalar state is very close to twice the physical fermion mass and $m_{PS} > 2m_f \gg m_\pi$. What is remarkable is the fact that the auxiliary field pion is considerably lighter than m_{PS} . This can be understood in terms of the mechanism of chiral symmetry restoration in 4-fermion interaction models whereby the disconnected contributions are responsible for making the pion light. We will provide numerical evidence for this below. If we measure the pseudoscalar propagator in the standard way from GG^\dagger we include only the connected contributions to the particle mass.

Fig. 8 shows the disconnected contribution to the Ward identity for a standard hybrid Monte Carlo simulation with $N = 3$ at zero chemical potential. For this simulation we

found that the signal for chiral condensate from the noisy estimator was relatively stable as shown in Fig. 9 giving $\langle\psi\bar{\psi}\rangle/m_q \simeq 40$, therefore we require that the sum of the connected and disconnected diagrams be of similar order so that Eqn. 5.1 is satisfied. The connected contribution was stable at a value of around 0.5 therefore the dominant contribution must come from the disconnected diagram. We found that the disconnected contribution was very noisy with large downward peaks. The data suggests that considering the connected contribution alone will never be sufficient to satisfy Eqn. 5.1.

We repeated our measurements for a non-zero chemical potential. We chose $\mu = 0.5$ thus ensuring that we were still in the phase of broken chiral symmetry. The results were consistent with those at zero chemical potential as one would expect.

As a consistency check observe that we expect the following relationships to hold from the equations of motion:

$$\bar{\psi}\psi = \frac{1}{g^2}\sigma \quad ; \quad \sum_y \bar{\psi}\varepsilon\psi(x)\bar{\psi}\varepsilon\psi(y) = \frac{1}{g^4}\frac{1}{V} \left(\sum_x \pi(x) \right)^2 \quad (5.5)$$

The first relationship has been checked and is satisfied by the simulation data. The second relation can also be verified. As seen in Fig 8 the characteristic peaks in the disconnected contribution are clearly correlated with the square of the pion field. We note that in the exact HMC study [6] the pion mass was obtained from the correlator of the auxiliary field π .

The disconnected contribution to the pion susceptibility gives a very noisy signal which suggests that a very long run would be required to equilibrate sufficiently to satisfy the lattice Ward identity.

VI. RELEVANCE OF GN STUDY TO QCD SIMULATIONS

The Glasgow Method for QCD is very similar to the method described in section III of this paper however because the QCD action is complex for ($\mu \neq 0$) we are restricted to generating the ensemble at $\mu_{upd} = 0$. Furthermore the relationship $\det M \hat{M} = \det M M^\dagger$ which we used in the lattice Gross-Neveu model does not hold for QCD at $\mu \neq 0$. We have seen in section IV that the GN model observables are sensitive to the choice of μ_{upd} and the most accurate results were obtained for $\mu_{upd} \simeq \mu_c$. Clearly it is impossible to simulate QCD at $\mu_{upd} \simeq m_p/3$ therefore we should be aware that very high statistics are likely to be required to obtain accurate observables from the Glasgow Method for QCD. It is still possible that the Lee-Yang zeros distribution will give a hint for μ_c even with moderate statistics and $\mu_{upd} = 0$. Since the Gross-Neveu model is a purely fermionic theory it is impossible to assess from our study what influence the gauge fields have in QCD dynamics in the context of Glasgow method reweighting [11].

In section V of this paper we have proved that the disconnected contribution to the Goldstone pion is dominant in the Gross-Neveu model. In QCD on the other hand we know that the pion has a dominant connected contribution which implies that

$$G_{ps}(t) \propto e^{-m_\pi t}$$

(c.f. eqn. 5.4) and this explains the origins of the early onset of the chiral transition in QCD associated with a light baryonic pion. The existence of the baryonic pion in the

Gross-Neveu model does not lead to an early onset of the chiral transition because it is the disconnected contributions which make the pion light i.e. the Goldstone mechanism is realised in a fundamentally different way.

VII. CONCLUDING REMARKS

In this paper we have found an example of a model where the inclusion of the chemical potential into the dynamics is essential to obtain exact results.

We have proved that the physical observables of the Glasgow Method are sensitive to the choice of μ_{upd} . The optimal choice for revealing critical behaviour is $\mu_{upd} \simeq \mu_c$, a choice which is impractical for QCD simulations. In QCD the pseudoscalar channel pole is formed from *connected* diagrams corresponding to $G_{+\mu}(t)G_{-\mu}^\dagger(t)$. A fermion pair with nonzero baryon charge (baryonic pion [5]) forms from a quark and a conjugate quark [3] (i.e. a fermion associated with M^\dagger but with the sign of μ reversed) and as a consequence the mass scale of the lightest baryon (m_{lb}) is $m_\pi/2$ not $m_p/3$.

This induces the unphysical early onset of chiral symmetry restoration in quenched QCD. In the full QCD it is conceivable that the phase of the determinant will eliminate the equality between quarks and conjugate quarks to allow us to recover the physical result $m_{lb} = m_p/3$. In principle the factor R_{rw} in the Glasgow algorithm should influence the observables to take account of the phase of the determinant. The Glasgow method QCD results [9] still suggest $m_{lb} \simeq m_\pi/2$. This is likely to be explained by ineffectiveness of the reweighting. The reweighting in the Gross-Neveu model has been shown to be ineffective and this is not surprising because in this case the statistical ensembles characterising the two phases are non-overlapping. The Glasgow method may however be more effective in models more sophisticated than Gross-Neveu and in other dynamical regimes such as at high temperature.

In 3d GN $U(1)$ the Goldstone mechanism is realised by a pseudoscalar channel pole formed from *disconnected* diagrams and the state $G_{+\mu}(t)G_{-\mu}^\dagger(t)$ yields a bound state of mass $2m_f(\mu = 0)$ which is considerably heavier than the pion. As a consequence even when we consider individual configurations in this model we find $\mu_o \simeq \mu_c \gg m_\pi/2$.

The different realisations of chiral symmetry breaking in the GN model and QCD have a simple physical origin. For QCD, a vector-like theory, like charges repel, so that light states only form between $q\bar{q}$ pairs (the pathologies in simulations of QCD with $\mu \neq 0$ occur because of the influence of conjugate quarks in the measure; in this case light states may be formed from qq^c pairs). In theories with Yukawa-like interactions such as the GN model, however, in the Born approximation all interactions are attractive, and thus one might expect light states made of $q\bar{q}$, qq and $\bar{q}\bar{q}$. Only the $q\bar{q}$ system has contributions from the disconnected diagram, however. As we have seen, binding in the connected channel is insufficient to make light states. Therefore we see a natural relation between the dominance of the disconnected diagram and the absence of light states made of two quarks in the spectrum.

It is also worth reconsidering why simulations of the GN model seem not to be afflicted with the problems observed in QCD. As we saw in Section II, the price of simulating with a real measure $\det(M^\dagger M)$ is that the model contains both “white” and “black” fermions with opposite axial charges. We might therefore worry about attractive interactions between white and black fermions and the possibility of light bound state in the $G_{+\mu}^{white}G_{+\mu}^{black}$ channel. The reason that no spurious onset at $\mu = m_\pi/2$ occurs, and that the GN simulations yield

results in good agreement with the mean field predictions, is intimately related to the fact that no light state occurs in this channel indeed the white-black interaction due to pion exchange in this model has the opposite sign and is thus *repulsive*: this is in contrast to the situation in gauge theories with real measure, where the interaction between quarks and conjugate quarks is attractive.

There are interesting parallels with the standard discussion of the Vafa-Witten theorem [23], forbidding the spontaneous breaking of global vectorlike symmetries such as isospin or baryon number in field theories with a positive definite measure in the path integral (this includes gauge theories with zero chemical potential but *not* Yukawa or GN models, for which the measure is in general complex). Vafa and Witten do in fact discuss a ‘white/black’ model with a real measure similar to ours, but with Yukawa couplings to a pseudoscalar field only. Their analysis does apply in this case, and a flavor-violating $\langle \bar{\psi}^{white} \psi^{black} \rangle$ condensate is forbidden, the reason being simply that the interaction between white and black particles is repulsive.

Once Yukawa couplings to scalar degrees of freedom are introduced, however, as in the GN model, the inequalities necessary to prove the Vafa-Witten theorem no longer hold. There appears to be no fundamental obstruction, therefore, to the generation of a baryon-number violating diquark condensate $\langle \psi^{white} \psi^{white} \rangle$ in this model, despite its measure being real; it has been recently suggested that such a condensate forms in QCD at high density [24]. A lattice study of this phenomenon is in progress [25].

VIII. ACKNOWLEDGEMENTS

We thank J.F. Lagaë for his comments related to measurement of the pion mass. MPL, SEM and SJH received support from EU TMR contract no. ERBFMRXCT97-0122. JBK thanks the National Science Foundation (NSF-PHY96-05199) for partial support.

REFERENCES

- [1] I. Barbour *et.al.*, Nucl. Phys. **B275**, 296 (1986).
- [2] C.T.H. Davies and E.G. Klepfish Phys. Lett. **256B**, 68 (1991).
- [3] M. Stephanov, Phys. Rev. Lett. **76**, 4472 (1996).
- [4] A. Gocksch, Phys. Rev. **D37** (1988) 1014.
- [5] M.-P. Lombardo, J.B. Kogut, D.K. Sinclair, Phys. Rev. **D54**, 2303 (1996).
- [6] S. Hands, S. Kim, J.B. Kogut, Nucl. Phys. **B442**, 364 (1995).
- [7] M.A. Halasz, A.D. Jackson, R.E. Shrock, M.A. Stephanov, J.J.M. Verbaarschot, hep-ph/9804290
- [8] I.M. Barbour, A.J. Bell, Nucl. Phys. **B372**, 385 (1992).
- [9] I.M. Barbour, J.B. Kogut, S.E. Morrison, Nucl. Phys. B (Proc. Suppl.) **B53**, 456 (1997).
- [10] N. Bilić, K. Demeterfi, B. Petersson, Nucl. Phys. **B377** 615 (1992).
- [11] I. Barbour, S.E. Morrison, E. Klepfish, J.B. Kogut, M.P. Lombardo, Phys. Rev. **D56**, 7063 (1997).
- [12] A. Hasenfratz and D. Toussaint, Nucl. Phys. **B371** (1992) 539
- [13] S. Duane, A.D. Kennedy, B.J. Pendleton and D. Roweth, Phys. Lett. **B195**, 216 (1987).
- [14] C.J. Burden and A.N. Burkitt, Europhys. Lett. **3**, 545 (1987)
- [15] S.J. Hands and J.B. Kogut, hep-lat/9705015. (1997).
- [16] P. Gibbs, Phys. Lett. **B172**, 53 (1986); P. Gibbs, Phys. Lett. **B182**, 369 (1986).
- [17] Susan E. Morrison, Nucl. Phys. **A642**, 269 (1998).
- [18] H. Matsuoka, M. Stone, Phys. Lett. **136B**, 204 (1984).
- [19] T.D. Lee, C.N. Yang, Phys. Rev. **87**, 404 (1952); Phys. Rev. **87**, 410 (1952).
- [20] S. Hands, A. Kocic, J.B. Kogut, Ann. Phys. **224**, (1993) 29.
- [21] B. Rosenstein, B.J. Warr and S.H. Park, Phys. Rev. **D39**, 3088 (1989).
- [22] S.J. Hands, A. Kocić and J.B. Kogut, Nucl. Phys. **B390**, 355 (1993).
- [23] C. Vafa and E. Witten, Nucl. Phys. **B234**, 173 (1984).
- [24] M. Alford, K. Rajagopal, F. Wilczek, Phys. Lett. **B422**, 247 (1998); R. Rapp, T. Schaefer, E.V. Shuryak, M. Velkovsky, Phys. Rev. Lett. **81**, 53, (1998).
- [25] S.J. Hands and S.E. Morrison, hep-lat/9807033.

FIGURES

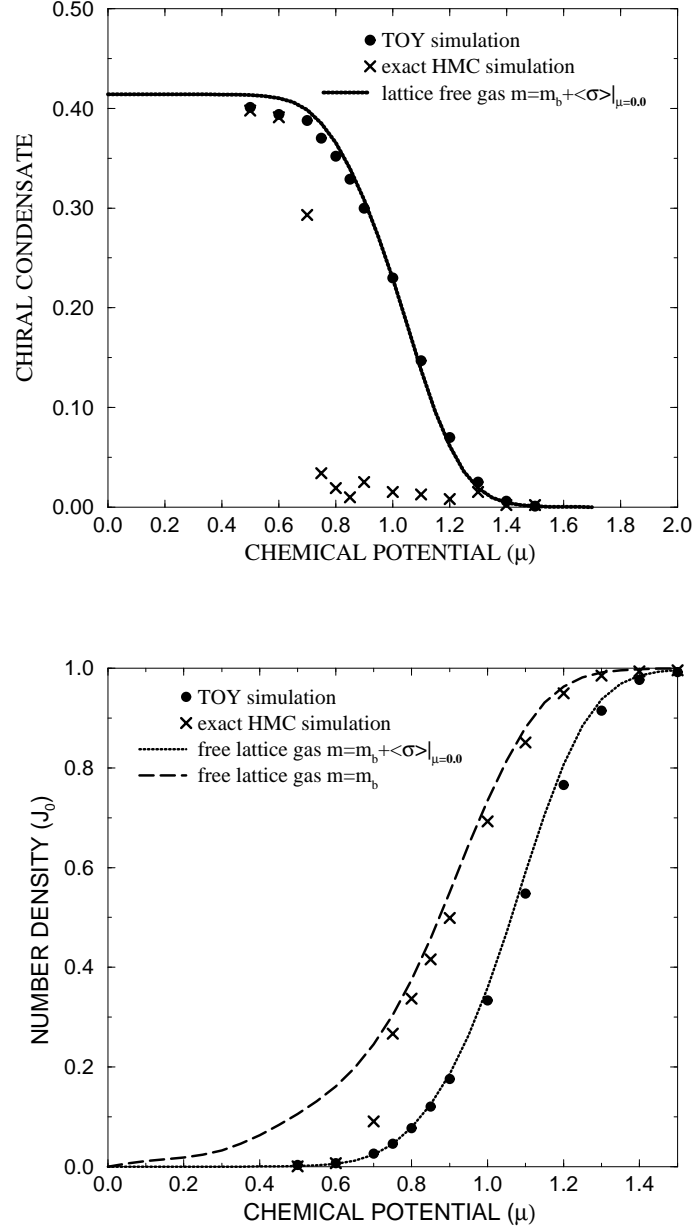


FIG. 1. $\langle \bar{\psi}\psi \rangle$ (upper) and J_0 in the full and Toy GN model at $\beta = 0.5$, $m_q = 0.01$, $L = 16$, $N = 3$. The data for the full model $\mu < 0.9$ are from [6]

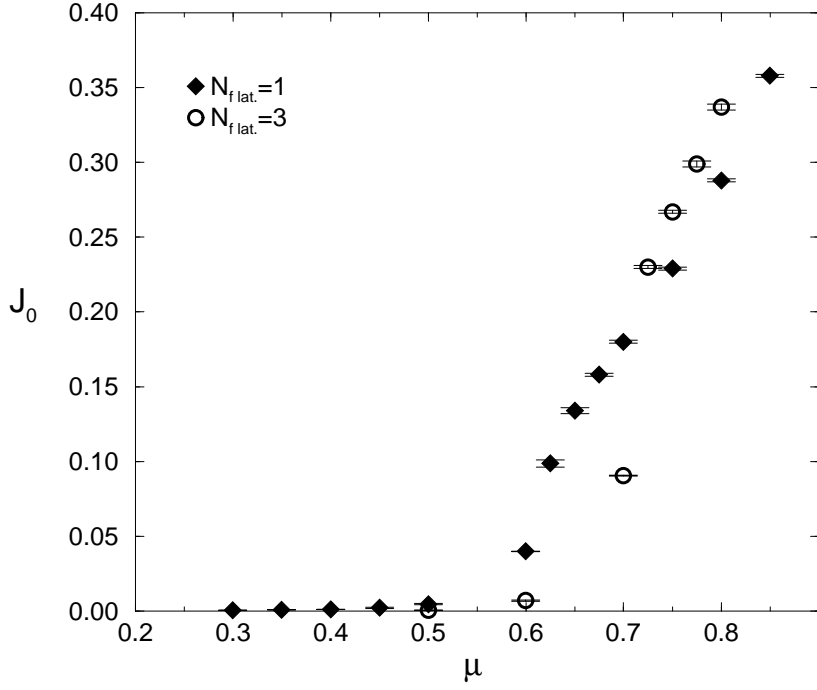


FIG. 2. Fermion number densities comparing exact hybrid Monte-Carlo simulations at $N = 1$ with $N = 3$ [6].

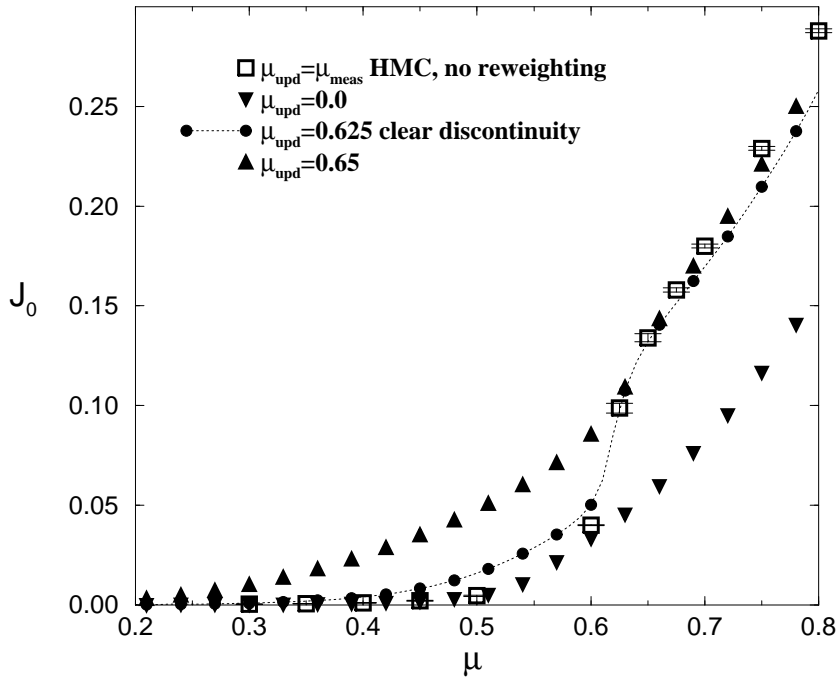


FIG. 3. Fermion number densities comparing simulations for three different values of μ_{ud} with the exact hybrid Monte-Carlo simulation on a 16^3 lattice with $1/g^2 = 0.5$, $N = 1$ and $m = 0.01$.

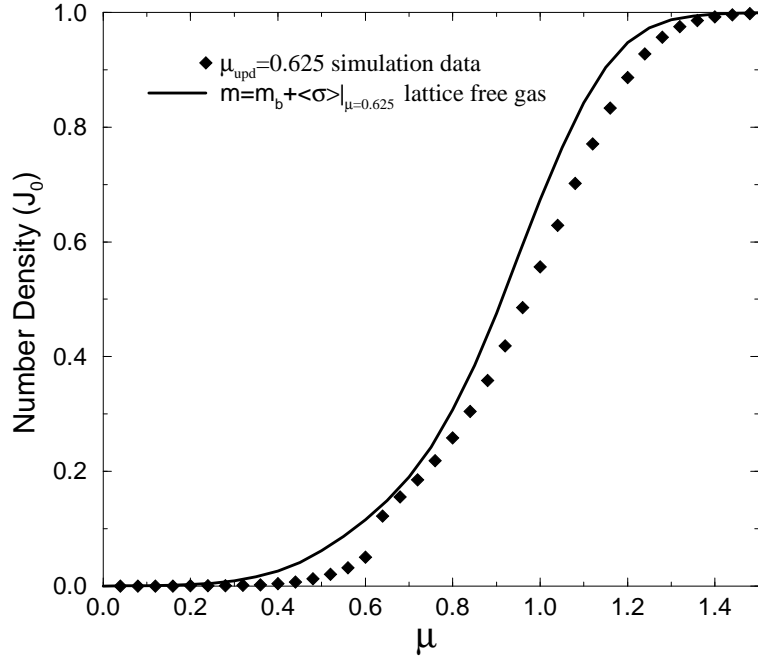
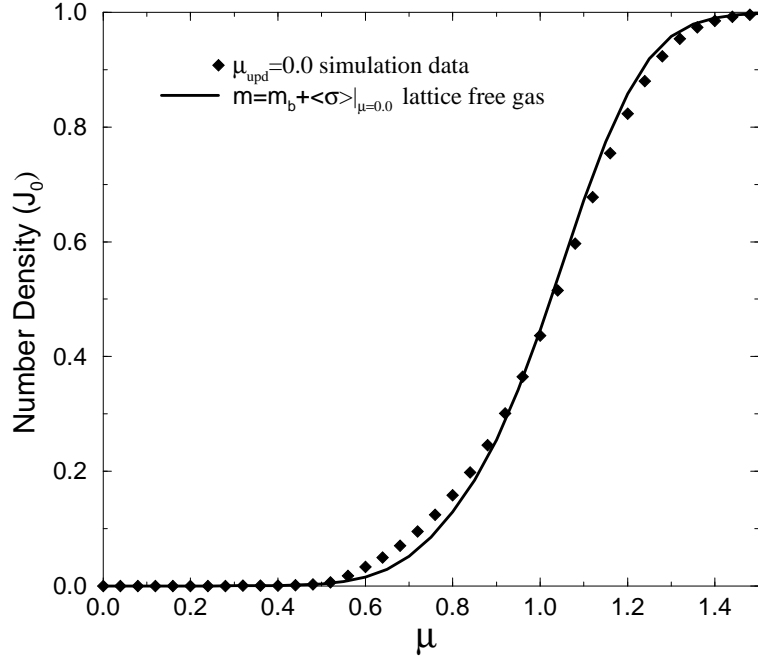


FIG. 4. Comparison of number densities (J_0) for free lattice gases of fermions of specified mass, m with the corresponding J_0 from Gross-Neveu simulations using the Glasgow method for $\mu_{\text{upd}} = 0.0$ (upper) and $\mu_{\text{upd}} = 0.625$ (lower) on a 16^3 lattice with $1/g^2 = 0.5$, $m = 0.01$ and $N = 1$.

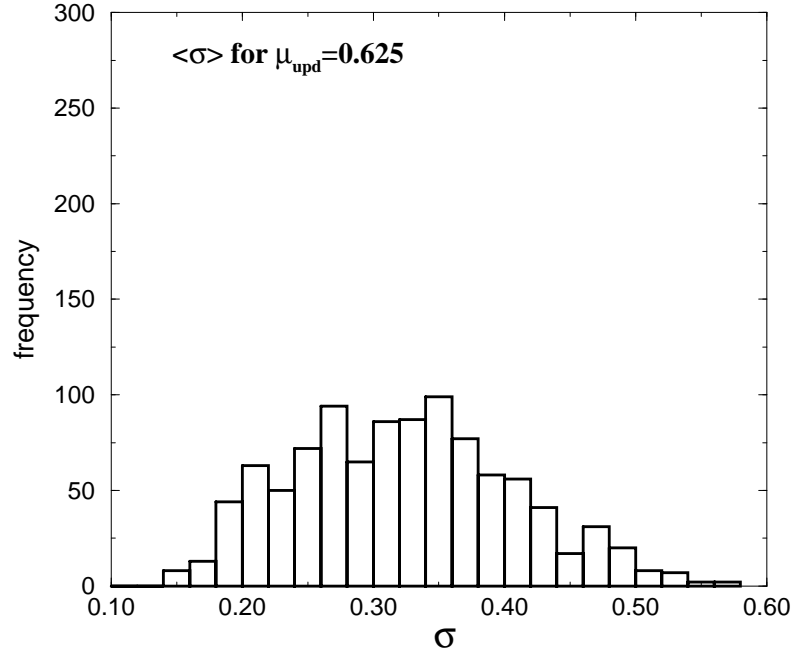
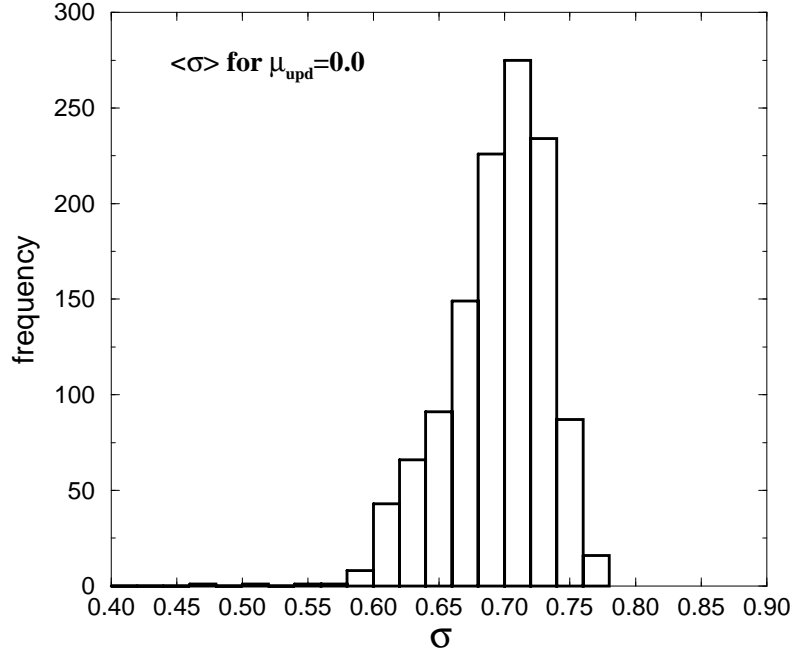
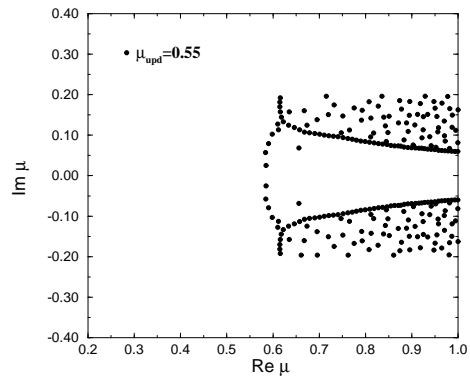
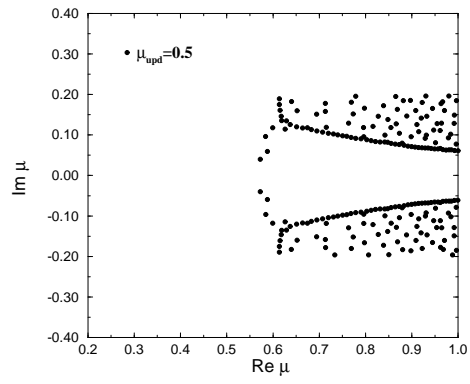
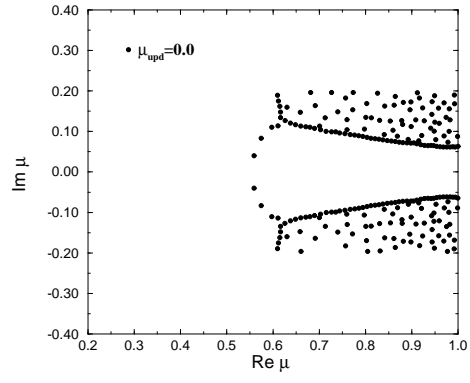


FIG. 5. Histograms for sigma field for $\mu = 0.0$ (upper) and $\mu = 0.7$ (lower) based on 1000 measurements on a 16^3 lattice with $1/g^2 = 0.5$, $m = 0.01$ and $N = 1$. The distribution is very sharply peaked in the $\mu = 0.0$ case and slightly broader for $\mu = 0.625$ which is close to μ_c .



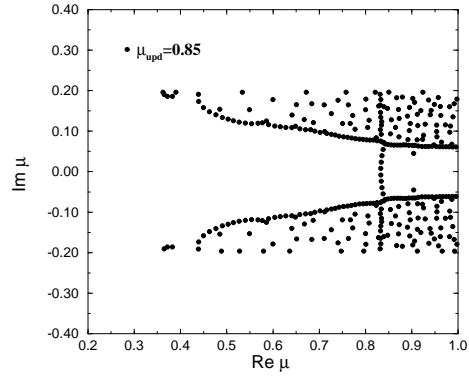
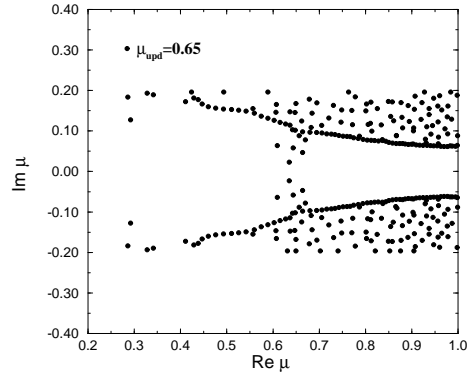
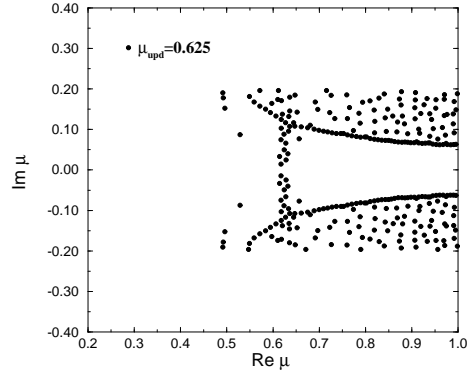


FIG. 6. Partition function zeros for six values of μ_{upd} . Simulations on 16^3 lattice with $N = 1$, $1/g^2 = 0.5$ and $m = 0.01$.

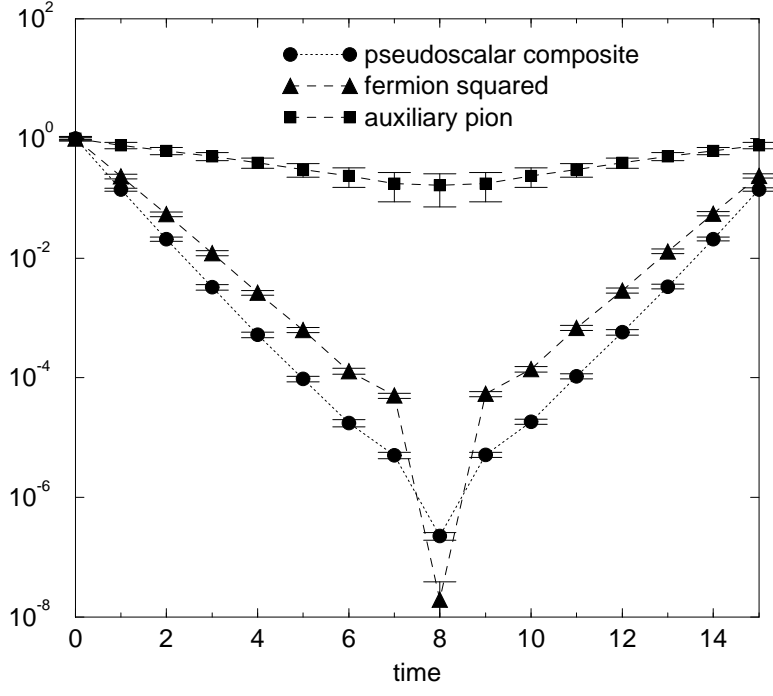


FIG. 7. Level ordering in 3d GN: from top to bottom, auxiliary pion propagators, fermion propagators squared, composite pseudoscalar propagator at $\beta = 0.5$, $m_q = 0.01$, $N = 3$ showing that $m_{PS} > 2m_f \gg m_\pi$.

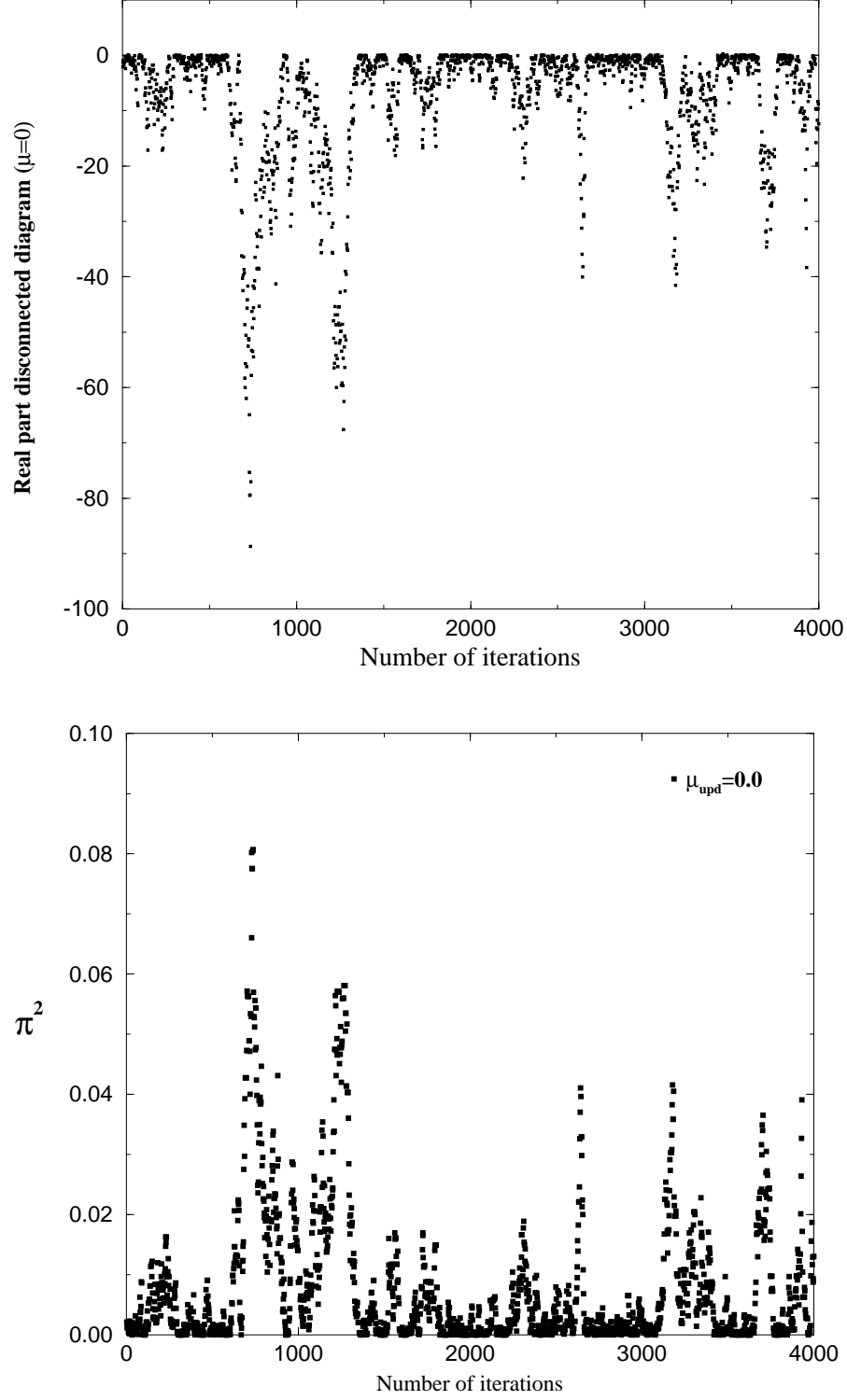


FIG. 8. Measurements at $\mu = 0.0$ showing the disconnected contributions to the pion susceptibility (upper) on a 16^3 lattice with $1/g^2 = 0.5$, $N = 3$ and $m = 0.01$ which we expect to be correlated with the auxiliary π field via an equation of motion.

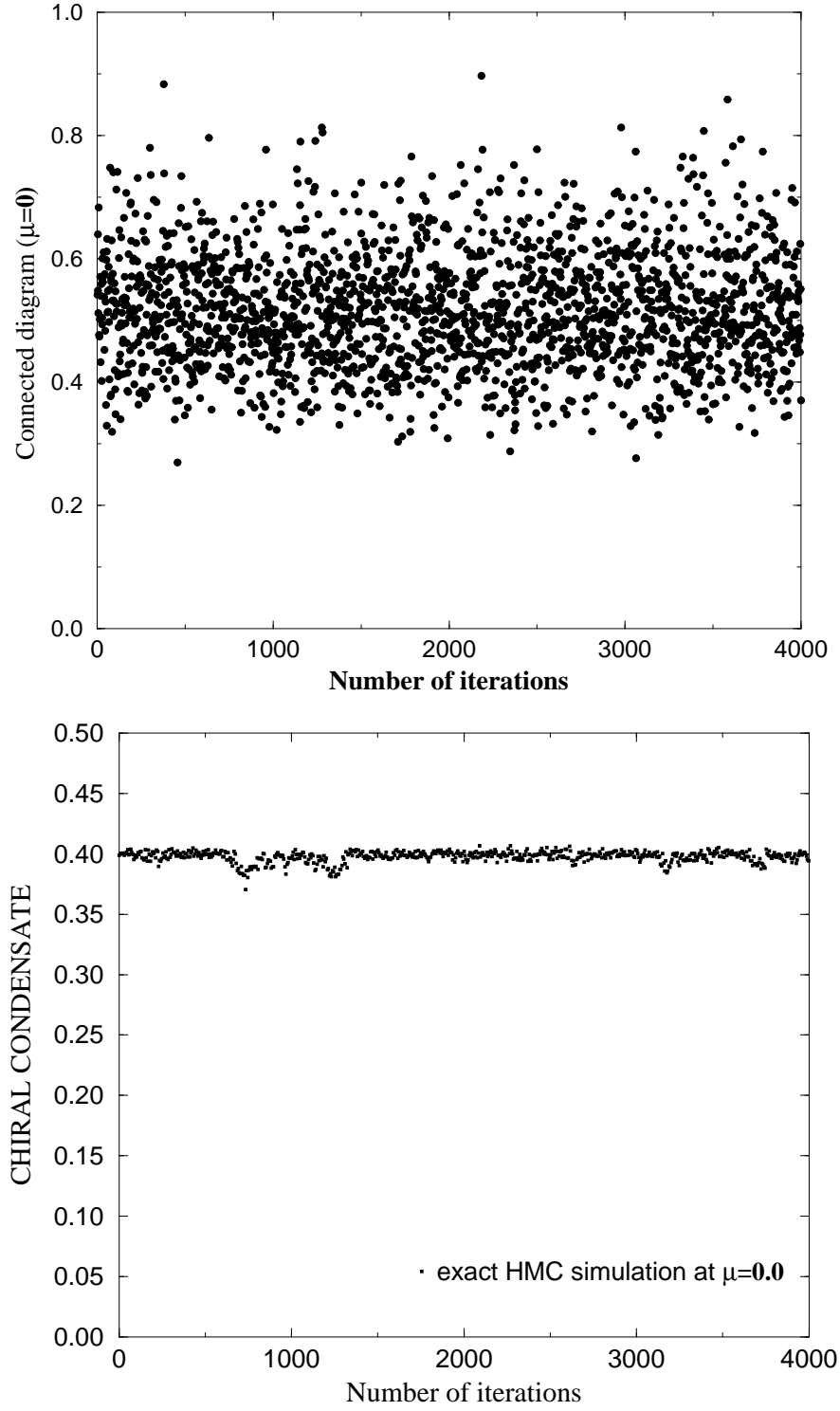


FIG. 9. Connected contribution to the pion susceptibility (upper) and the chiral condensate (lower) at $\mu = 0.0$ on 16^3 lattice with $1/g^2 = 0.5$, $N = 3$ and $m = 0.01$.

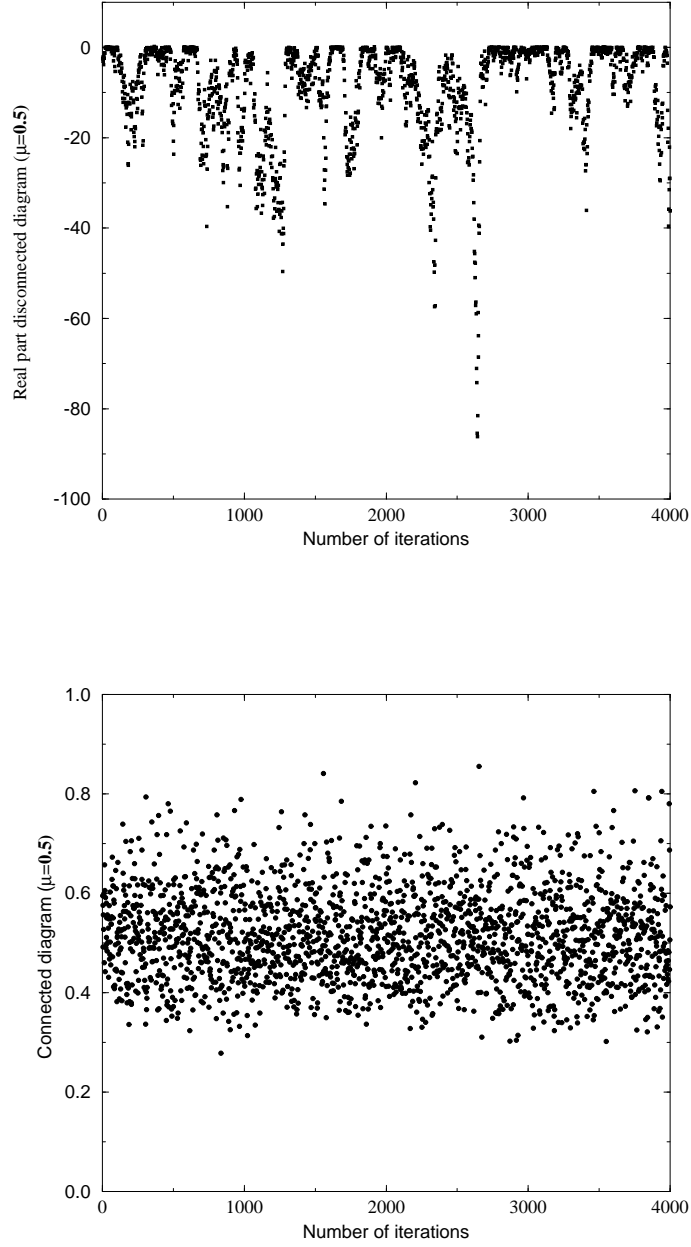


FIG. 10. Measurements at $\mu = 0.5$ showing the relative magnitudes of the disconnected (top) and the connected (bottom) contribution to the pion on a 16^3 lattice with $1/g^2 = 0.5$, $N = 3$ and $m = 0.01$.